J. Fluid Mech. (1975), *vol.* 67, *part* 3, *pp.* 539–559
Printed in Great Britain

Fine-structure of energy spectra of velocity fluctuations in the transition region of a two-dimensional wake

By HIROSHI SATO AND HIRONOSUKE SAITO
Institute of Space and Aeronautical Science, University of Tokyo, Japan

(Received 22 October 1973 and in revised form 2 April 1974)

Measurements of the fine-structure of the energy spectrum of the velocity fluctuations were made in the transition region of a two-dimensional wake. Line and continuous spectra were determined separately with a high-selectivity band-pass filter. The transition was initiated by an external sinusoidal sound. The sound-induced periodic fluctuation and the natural random fluctuation in the wake were added and a system of line and continuous spectra was formed. Higher harmonics of the periodic component were produced by the nonlinear interaction. As a result of the interaction between discrete and continuous components, a continuous spectrum was generated at low wavenumbers. A simple model for the interaction is proposed. The evolution of the spectrum is explained by three fundamental rules concerning the nonlinear interaction between spectral components: (i) the growth of a spectral component is suppressed by the presence of another strong component, (ii) mutual interaction is more effective when the amplitudes of interacting components are closer, and (iii) a stronger interaction takes place between components of closer wavenumbers. The randomization of the regular fluctuation is properly expressed as the growth of the 'randomness factor', the ratio of the energy of the random components to the total fluctuation energy.

1. Introduction

The laminar–turbulent transition of free shear flows initiated by a small amplitude disturbance consists of three elementary processes. The first is the selective amplification of the disturbance. If the wavenumber of the disturbance is appropriate, the disturbance grows exponentially in the flow direction. So long as the amplitude of the disturbance is small, there are no interactions between fluctuations of different wavenumber. Experimental results on the growth rate, phase speed and other properties of small amplitude fluctuations are in good agreement with predictions of linearized stability theory (Sato & Kuriki 1961). The second process is the nonlinear interaction of the amplified, large amplitude fluctuations. It leads to the reduction of the growth rate, the production of harmonics and the distortion of the mean-velocity distribution. If there are two fluctuations of different wavenumber, components whose wavenumbers are the sum and difference of the two wavenumbers are generated.

Although there are many experimental results on the nonlinear interactions in various flow fields (Klebanoff, Tidstrom & Sargent 1962; Sato 1970; Miksad 1972, 1973), existing nonlinear theories explain only a part of them. The last and most significant process in the transition is the randomization. The nonlinear interaction of various fluctuations is a deterministic process; in other words, if interacting fluctuations are periodic, the periodicity is not destroyed by the interaction. On the other hand, turbulence is random. Therefore, the randomization of periodic fluctuations must take place as the final process of transition.

The randomization process is most appropriately described in terms of the evolution of the energy spectrum. If the initial disturbance is a fluctuation with a single frequency, the corresponding energy spectrum is a single line spectrum. The intensity of the line spectrum increases exponentially in the linear region of transition and the nonlinear interaction results in the production of harmonic line spectra. The spectrum of the turbulent fluctuation, on the other hand, is continuous. Therefore, the randomization process corresponds to the evolution from the line spectra to the continuous spectrum. An example of the broadening of discrete mode frequencies was given by Lashinsky (1968) both theoretically and experimentally. But so far there is no general theory for the randomization. Existing experimental results on the energy spectra in the transition region are not satisfactory, because in these experiments line and continuous spectra have not been separated clearly. For the quantitative discussion of the randomization process we have to know the '*fine-structure*' of spectra; namely, line and continuous spectra must be separated with sufficient accuracy. This is the reason why we started measurements of the fine-structure of energy spectra in the transition region. The present paper includes experimental results in the two-dimensional wake behind a flat plate and discussions on the randomization process.

2. Experimental arrangement and procedure

Wind tunnel, hot-wire anemometer and band-pass filter

The whole experiment was carried out in the 60 × 60 cm Low-Turbulence Wind-Tunnel at the Institute of Space and Aeronautical Science, University of Tokyo. A thin aerofoil (of chord 30 cm, span 60 cm, maximum thickness 3 mm and thickness at the trailing edge ~ 0·2 mm) was placed parallel to the uniform flow in the test section and a two-dimensional symmetrical laminar wake was generated behind the plate. Mean and fluctuating velocities were measured by a constant-temperature hot-wire anemometer. Figure 1 illustrates the layout of the test section. A loudspeaker at the exit of the test section was used for introducing sound into the wake. The X axis is in the flow direction and the Y axis is perpendicular to the plate. Details of the tunnel, the wake-producing plate, the loudspeaker, the hot-wire equipment, etc., may be found in a previous paper (Sato 1970). The free-stream velocity was fixed at 10 m/s.

The signal from the hot-wire amplifier was analysed by a band-pass filter. The discrimination of line spectra from the continuous part was accomplished by a filter of extremely high selectivity. The newly constructed filter employs a

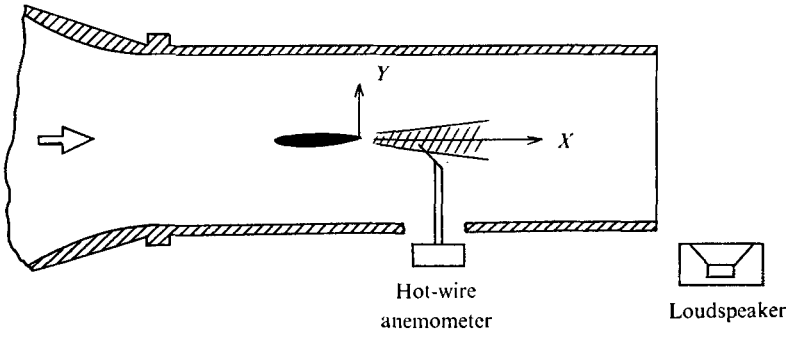

FIGURE 1. Layout of test section.

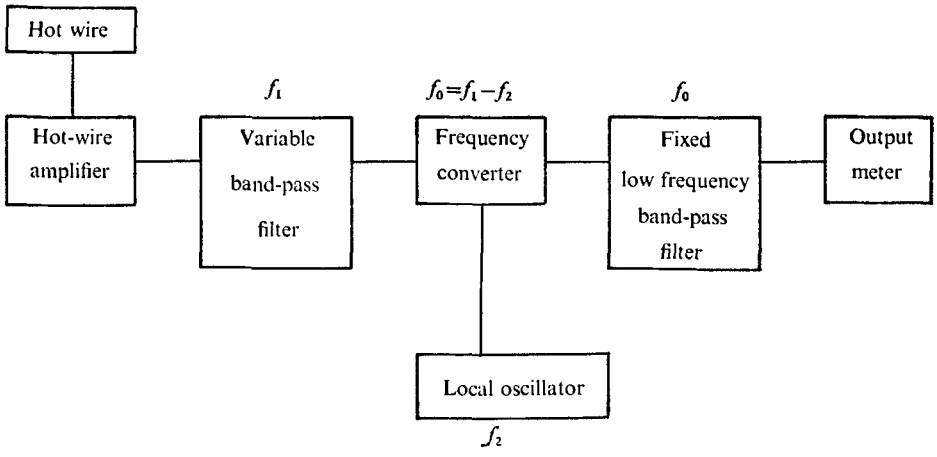

FIGURE 2. Block diagram of high-selectivity band-pass filter.

heterodyne circuit, whose block diagram is shown in figure 2. The signal from the hot-wire amplifier is fed to a conventional band-pass filter which is tuned to the frequency f_1. The selectivity of this filter, defined by $f_1/\Delta f$, Δf being the bandwidth of 6 db attenuation, is about 30. The filtered signal is mixed with a sinusoidal signal from a local oscillator of frequency f_2 and converted to a signal of frequency $f_0 = f_1 - f_2$. The frequency of the second filter is fixed at f_0, which is around 30 Hz. With a large value of f_1/f_0 a high selectivity was obtained. The spectrum was determined by changing both f_1 and f_2. The attenuation characteristics of the whole filter system are -23 db at ± 5 Hz, -29 db at ± 10 Hz and -44 db at ± 40 Hz difference from the tuned frequency. This implies that the influence of an adjacent strong discrete component on the measurement of a weak continuous spectrum is small. Corrections for such an influence were made by using the filter characteristics.

Artificial small amplitude fluctuations

The root mean square of the longitudinal component of the residual fluctuation in the test section was about 0·05% of the free-stream velocity. Although a precise measurement of the energy spectrum of the fluctuation was not possible

because of the smallness of the signal, it was ascertained that there was no predominant discrete component in the wave form. A so-called natural transition was originated by the fluctuation. On the other hand, if we introduce sound of a single frequency into the wake, the spectrum of the velocity fluctuation induced by the sound is a line spectrum. The mechanism of transition originated by the induced fluctuation might be different from that of natural transition. Since the amplitude and frequency of the sound-induced fluctuation can be controlled, the sound-induced transition is better defined. In the present experiment a transition of this type was investigated in detail. The frequency of the sound was 600 Hz. At this frequency the linear growth rate of the induced fluctuation is maximum under the present experimental conditions.

The reproducibility of the experiment was assured by adjusting the intensity of the sound so that the root-mean-square induced velocity fluctuation at a reference point in the wake, $X = 10\,\text{mm}$, $Y = 0{\cdot}5\,\text{mm}$, was $0{\cdot}5\,\%$ of the free-stream velocity. The level of the natural fluctuation at this point without sound was about $0{\cdot}05\,\%$. Since the sound-induced fluctuation in the uniform free stream was about $0{\cdot}005\,\%$, the above-mentioned r.m.s. value of the fluctuation at the reference point is a result of growth by a factor of about 100 in the wake. Although sound induces velocity fluctuations everywhere in the flow, the fluctuation induced near the trailing edge of the plate grows most. Therefore, the actual effect of sound is very localized and we may consider the initial disturbance to exist only around the trailing edge.

3. Experimental results

Mean flow

Distributions of the mean velocity at various X stations in the presence of 600 Hz sound are shown in figure 3, in which the mean velocity U is normalized by the free-stream velocity U_0. The distribution changes from an almost Blasius profile at $X = 5\,\text{mm}$ to a typical distribution for a turbulent wake at $X = 1000\,\text{mm}$. We notice two interesting facts from the figure. One is the decrease of the velocity on the centre-line from $X = 60$ to $120\,\text{mm}$ in contrast to the expected gradual increase to the free-stream velocity. The other is the overshoot of U/U_0; namely, U exceeds U_0 at around $Y = \pm 5\,\text{mm}$ at $X = 120\,\text{mm}$. These features were found previously in natural transition and it was clarified that they resulted from the nonlinear interaction between the large amplitude velocity fluctuation and the mean flow (Sato 1970).

Streamwise variations of the velocity U_c on the centre-line and the half-value breadth b are shown in figure 4. Results in natural transition are added for comparison. In both the natural and sound-induced cases the general trends of the streamwise variations are the same. The differences are that sharp increases of U_c and b take place at smaller X in the presence of sound. At large X, U_c and b in natural transition are larger. In the presence of sound, both U_c and b remain almost unchanged between $X = 150$ and $600\,\text{mm}$. This is an indication of the establishment of nonlinear equilibrium in the region.

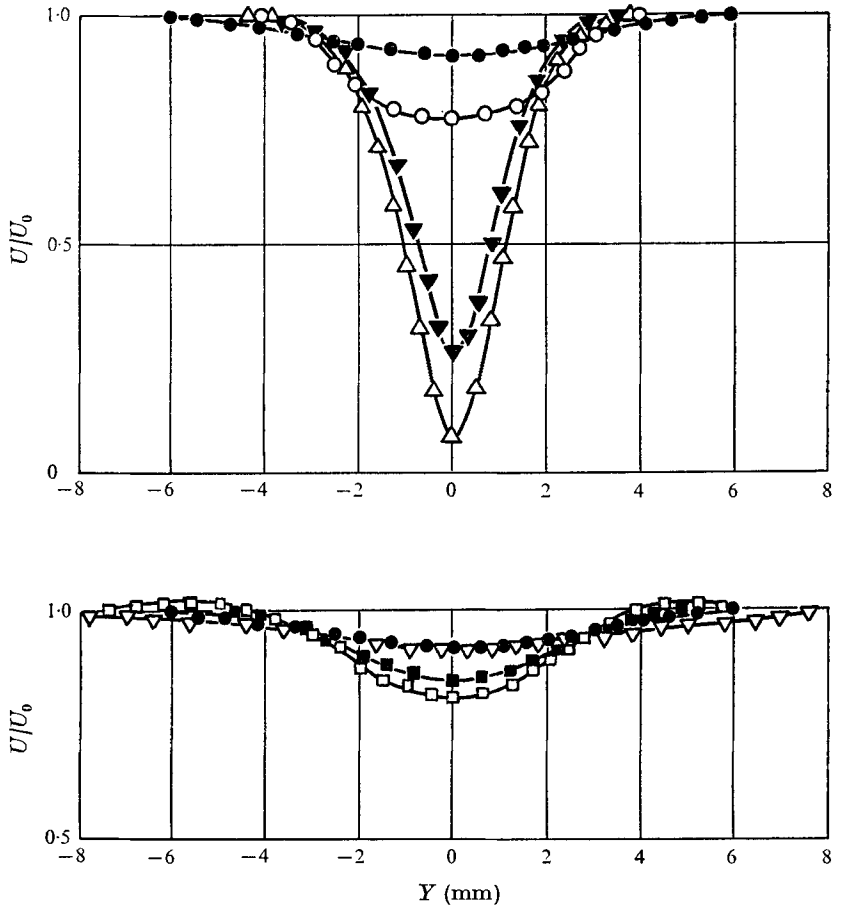

FIGURE 3. Mean-velocity distributions with 600 Hz sound. $U_0 = 10$ m/s. △, $X = 5$ mm; ▼, $X = 20$ mm; ○, $X = 40$ mm; ●, $X = 60$ mm; □, $X = 120$ mm; ■, $X = 400$ mm; ▽, $X = 1000$ mm.

Velocity fluctuations

Distributions of the root-mean-square u fluctuation for sound-induced transition are shown in figure 5. The fluctuation grows from a small value at $X = 5$ mm to $(\overline{u^2})^{\frac{1}{2}}/U_0 = 0{\cdot}15$ at $X = 40$ mm and gradually decreases downstream. The growth from $X = 5$ to 20 mm was found to be exponential. At small X the distribution has two peaks and the Y positions of the two peaks roughly coincide with the locations of the maxima of $\partial U/\partial Y$ at each X station. At large X the distribution is rather flat. The fact that $(\overline{u^2})^{\frac{1}{2}}$ is maximum at $X = 40$ mm is not an indication of the onset of turbulence. The wave form of the fluctuation around $X = 40$ mm is still regular and periodic. Randomness in the wave form first appears at around $X = 800$ mm. The maximum root-mean-square value $(\overline{u^2})^{\frac{1}{2}}_{\max}$ at each X station is plotted against X in figure 6. The streamwise variation of $(\overline{u^2})^{\frac{1}{2}}_{\max}$ is closely related to the streamwise distributions of U_c and b. In both figures 4 and 6 sharp increases take place at $x < 50$ mm and the remarkable increase of b starting at

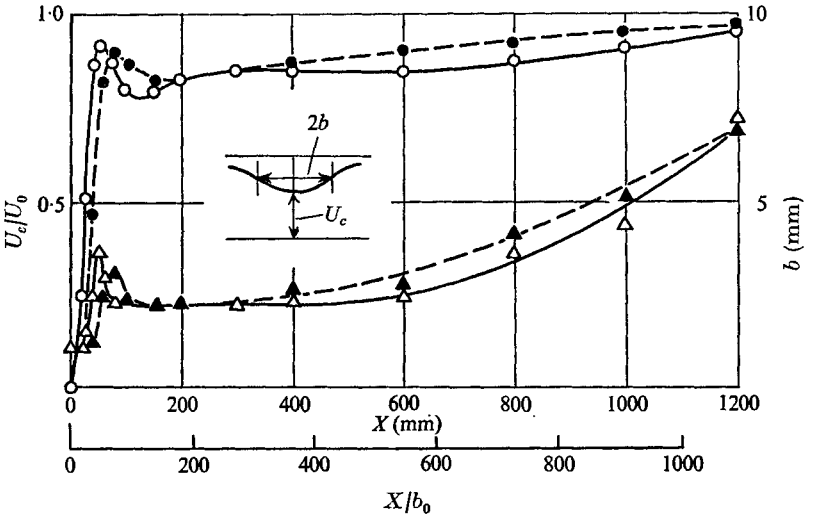

FIGURE 4. Streamwise variations of velocity U_c on the centre-line and half-value breadth b. ○, U_c/U_0 with 600 Hz sound; ●, U_c/U_0 in natural transition; △, b with 600 Hz sound; ▲, b in natural transition. b_0 = half-value breadth at $X = 0$.

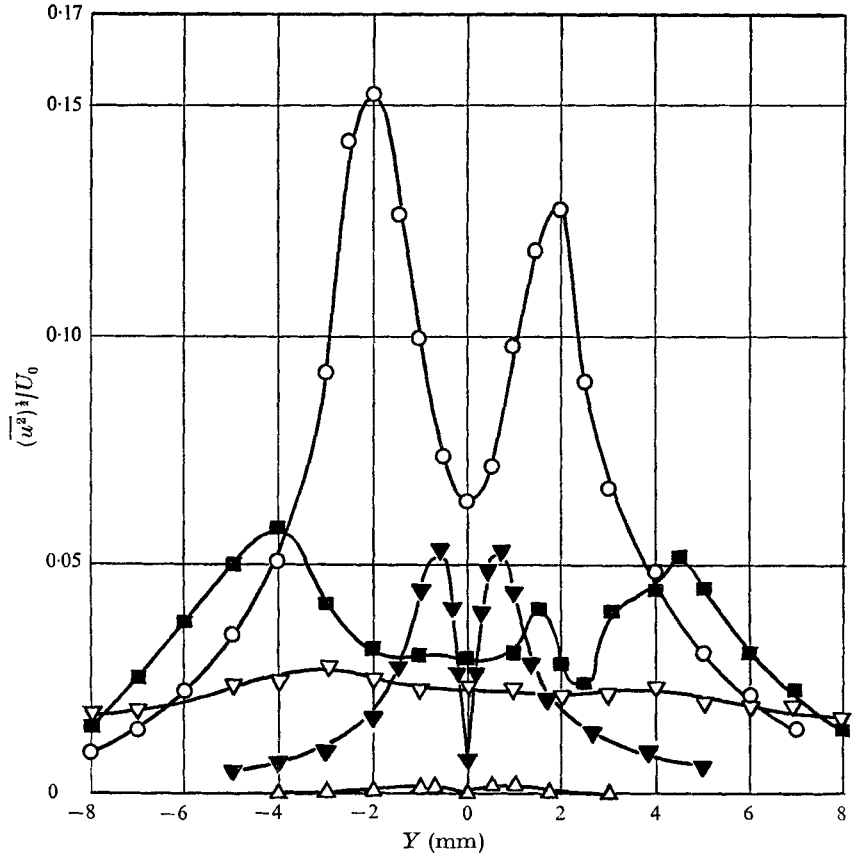

FIGURE 5. Fluctuation-intensity distributions with 600 Hz sound. △, $X = 5$ mm; ▼, $X = 20$ mm; ○, $X = 40$ mm; ■, $X = 400$ mm; ▽, $X = 1000$ mm.

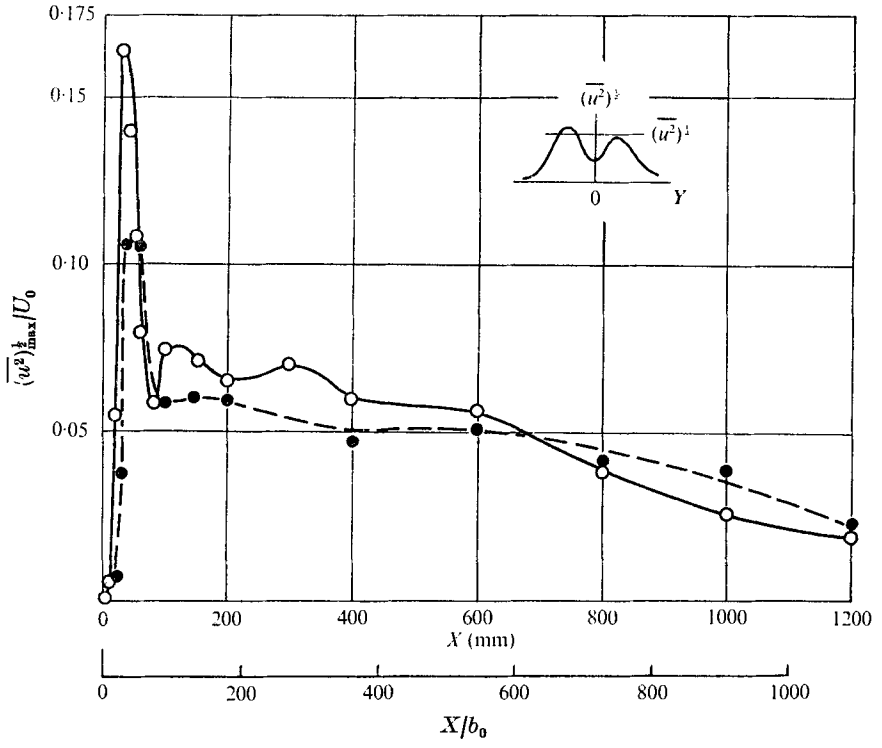

FIGURE 6. Streamwise variations of maximum value of fluctuation intensity at each X station. ○, with 600 Hz sound; ●, natural transition. b_0 = half-value breadth at $X = 0$.

around $X = 600$ mm corresponds to the decrease of the fluctuation intensity in figure 6. Intense fluctuations do not necessarily lead to a rapid widening of the wake. Fluctuations at large X are more random although they are weak. These random fluctuations are effective in widening the wake. The curve for natural transition added for comparison in figure 6 is slightly lower at small X. The two curves become closer at large X.

Wave forms of the velocity fluctuation are reproduced in figure 7. At $X = 20$ mm, $Y = 0{\cdot}5$ mm the wave form is sinusoidal with a frequency of 600 Hz. On the centre-line at $X = 60$ mm second harmonics are dominant. The wave forms at three X stations, $X = 60$, 150 and 600 mm, are very much alike. They are periodic waves of the same frequency with strong second harmonics on the centre-line. This is another indication of nonlinear equilibrium in the region between $X = 150$ and 600 mm. In wave forms at $X = 800$ mm both periodic and random components exist. At $X = 1200$ mm the wave forms are quite irregular and random, that is, a turbulent wake is established there. The randomization process takes place between $X = 600$ and 1200 mm. Wave forms at $X = 600$ mm in natural transition are shown in figure 8 for comparison. They are more irregular than the corresponding wave forms at the same X station in the presence of sound. Apparently, the sinusoidal sound makes fluctuations regular and delays the transition.

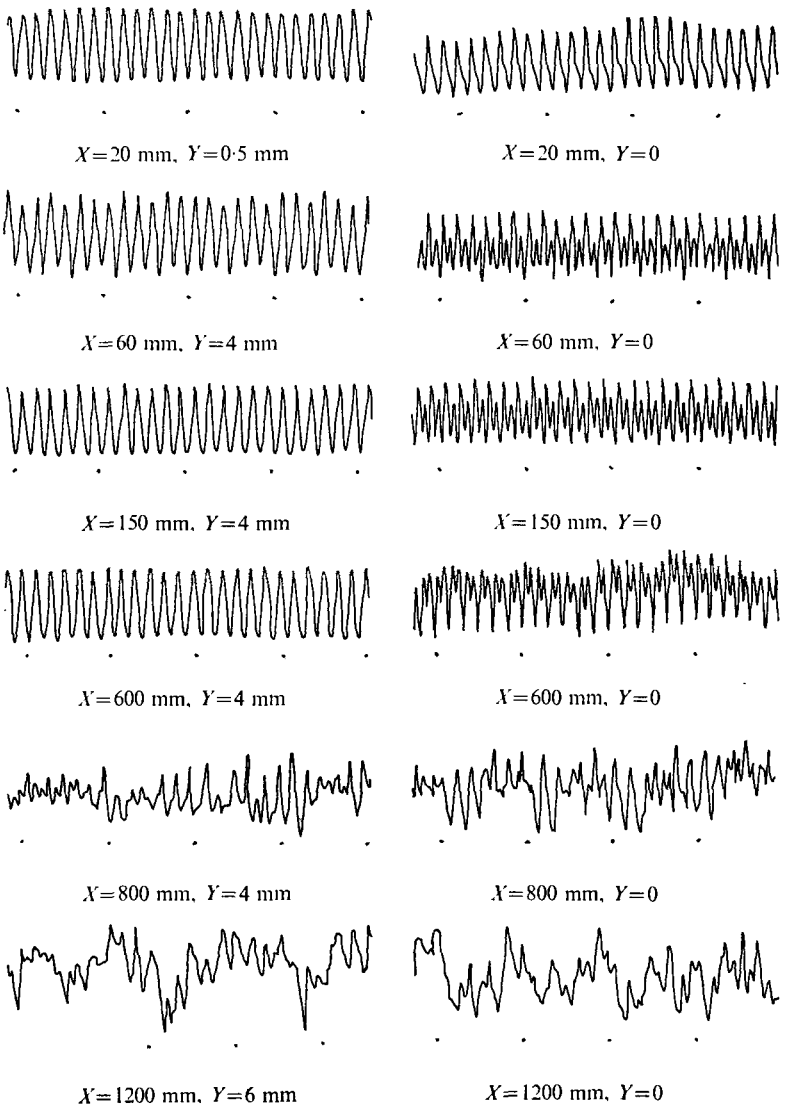

FIGURE 7. Wave forms of u fluctuation with 600 Hz sound. Velocity increases upwards. Time increases from left to right; interval between dots, 0·01 s.

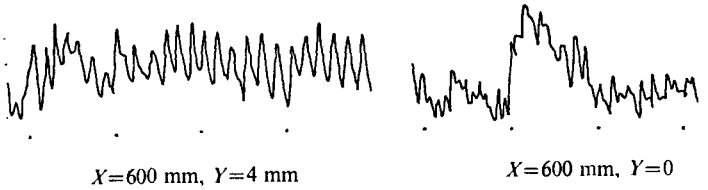

FIGURE 8. Wave forms of u fluctuation in natural transition.

Energy spectra

The velocity fluctuation in the transition region includes both periodic and random components. The energy $\overline{u^2}$ of such a fluctuation is decomposed into

$$\overline{u^2} = \sum_j \overline{u_j^2} + \overline{u^2} \int_0^\infty E(k)\, dk,$$

in which $\overline{u_j^2}$ represents the discrete energy at the wavenumber k_j (line spectrum) and $E(k)\,dk$ denotes the spectral density between k and $k+dk$ (continuous spectrum). By this definition,

$$\int_0^\infty E(k)\, dk \neq 1.$$

Theoretically, the separation of line and continuous spectra is possible by considering an ideal band-pass filter which has a uniform gain between k and $k+dk$. If the output energy from the filter is proportional to dk, we calculate the proportionality constant for $E(k)$. On the other hand, if the output signal has a definite energy in the limit $dk \to 0$, we select a line spectrum at k. Experimentally, the separation is accomplished by comparing the measured spectrum with the characteristics of a narrow-band filter. Since $\overline{u_j^2}$ and $E(k)$ differ in dimension, they will be shown separately.

Line spectra

Measurements of line spectra were made at about 40 mesh points in the X, Y plane in the wake. Since it is impossible to reproduce all the spectra, the streamwise variations of the spectra at two Y positions are illustrated. One is along the centre-line ($Y = 0$, figure 9*a*) and the other is at $Y = 4$ mm, which roughly corresponds to the point of maximum $\overline{u^2}$ at each X station (figure 9*b*). The ordinates in these two figures are the mean squares of discrete components as fractions of U_0. The numbers in parentheses on the abscissae denote the order of the harmonics, namely, (1), (2), (3), ..., correspond to the fundamental, second harmonics, third harmonics and so on. At $X = 60$ mm we can count up to six harmonics. In figure 9 (*a*) the second-harmonic component is dominant at $X < 600$ mm and, generally speaking, even-order harmonics are stronger than odd-order harmonics. On the other hand, at off-centre positions (figure 9*b*) harmonics of odd orders predominate. Measurements of Y distributions of the intensities of discrete components reveal that on the centre-line even-order harmonics have maximum values, whereas odd-order harmonics have minima. Higher harmonics decay faster and at $X = 1000$ mm only the fundamental and second harmonics are observed. The spectra between $X = 150$ and 600 mm do not change much. This is another indication of the equilibrium nature of the region. A remarkable decrease in line spectra takes place between $X = 800$ and 1000 mm. At $X = 1200$ mm the intensity of the fundamental component is only about 10^{-4} times the intensity at $X = 60$ mm. The transition region ends and a turbulent wake is established there.

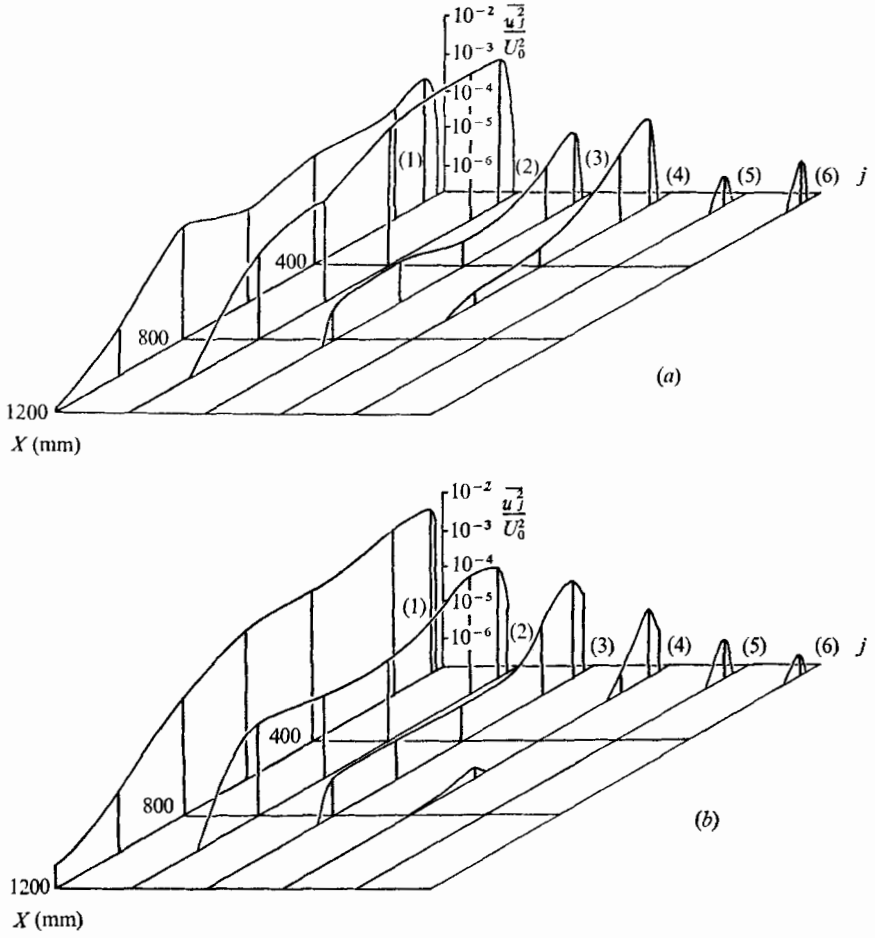

FIGURE 9. Streamwise variation of various harmonic components at (*a*) $Y = 0$ and (*b*) $Y = 4$ mm with 600 Hz sound. j = order of harmonics.

There are no subharmonic components. This is in contrast to the findings in the asymmetrical shear layer, in which subharmonics are clearly observed (Sato 1959; Browand 1966; Miksad 1972).

Continuous spectra

At small X the continuous spectrum is very weak compared with the discrete components. For instance, the wave form at $X = 150$ mm, $Y = 4$ mm in figure 7 is regular and periodic and the energy contained in the continuous spectrum is less than 1% of the total energy. Figure 10 (*a*) shows the continuous spectrum at this point. The abscissa variable is the wavenumber k, which is given by

$$k = \text{fluctuation frequency/free-stream velocity.}$$

The ordinate variable, the spectral density $E(k)$, has an arbitrary scale but all spectral densities shown in this section have the same scale so that the relative

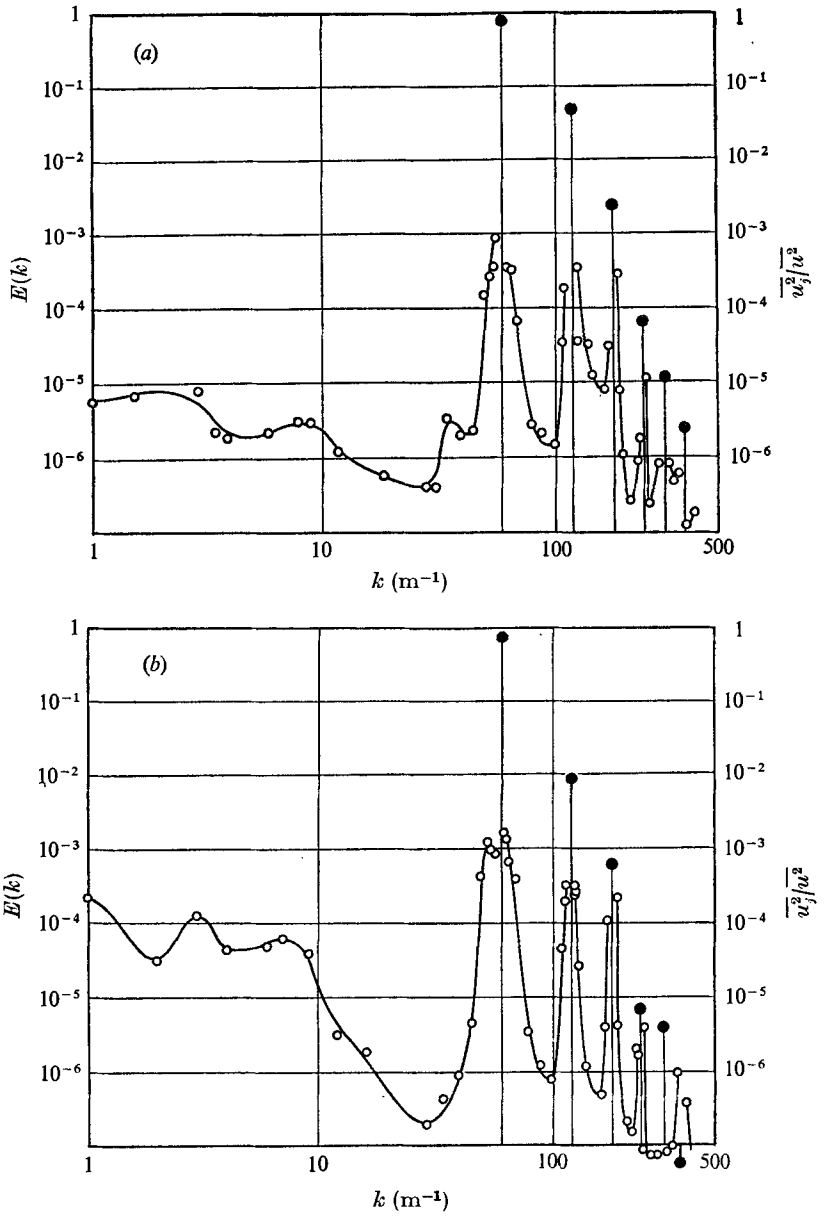

FIGURES 10(*a*, *b*). For legend see p. 551.

intensities at various points are expressed correctly. Discrete components are also shown in the figure by solid circles as fractions of the total energy. We notice in the figure that most of the random energy is contained in 'humps' around discrete components. This combination of the discrete component and the hump corresponds to the random variation of the amplitude of a periodic fluctuation. To use the terminology of communication technology, line spectra correspond to carrier waves and humps to side bands. That is, the fundamental 600 Hz component

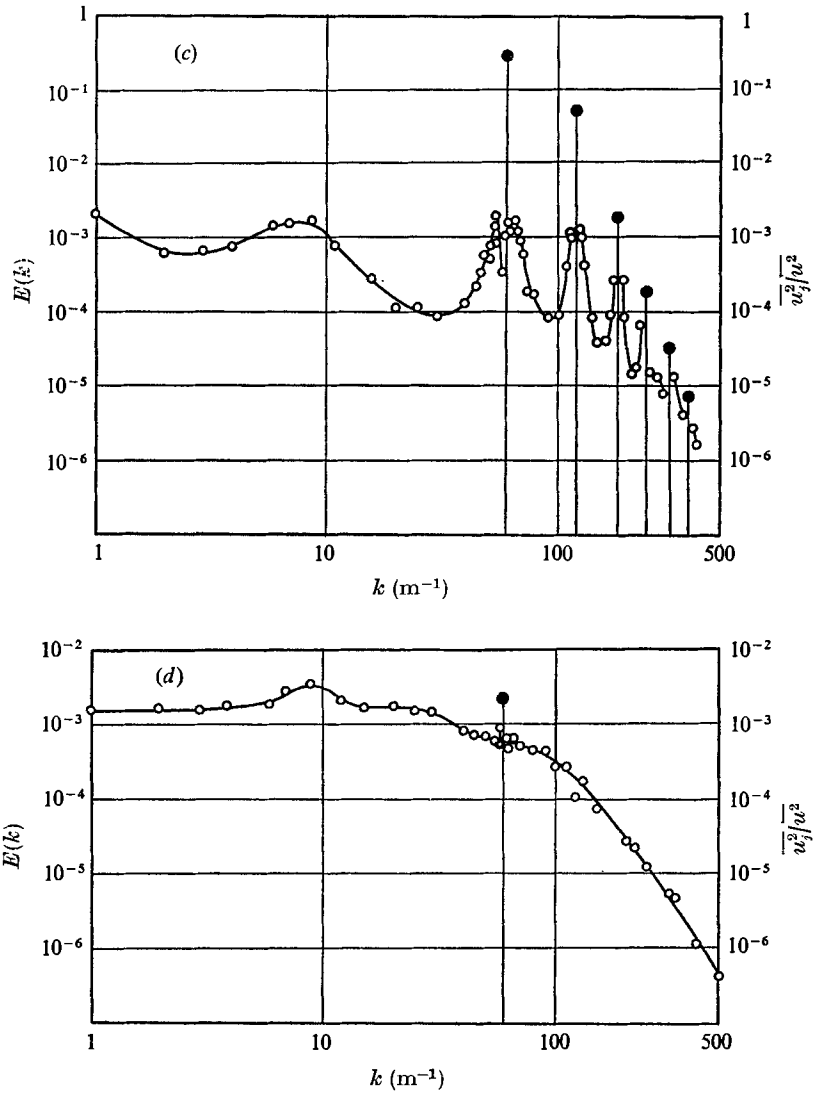

FIGURES 10(*c*, *d*). For legend see facing page.

($k = 60\,\mathrm{m}^{-1}$) and higher harmonics are modulated by slow irregular fluctuations. The maximum frequency of the side band is about 200 Hz ($k = 20\,\mathrm{m}^{-1}$). This range of frequency of the modulating signal is common to all harmonics. The energy at low wavenumbers is extremely small. Spectra measured at different Y positions at this X station are alike.

Figure 10 (*b*) shows the spectrum at $X = 400\,\mathrm{mm}$, $Y = 4\,\mathrm{mm}$. The energy contained in the continuous part at this point is about 30% of the total energy. By comparing this with figure 10 (*a*) we find a remarkable increase at low wavenumbers: between $k = 1$ and $10\,\mathrm{m}^{-1}$. Changes in the height and width of the humps in the two figures are small. Changes at valleys between humps are also small. The spectrum at $X = 800\,\mathrm{mm}$, $Y = 4\,\mathrm{mm}$ (figure 10*c*) indicates a further

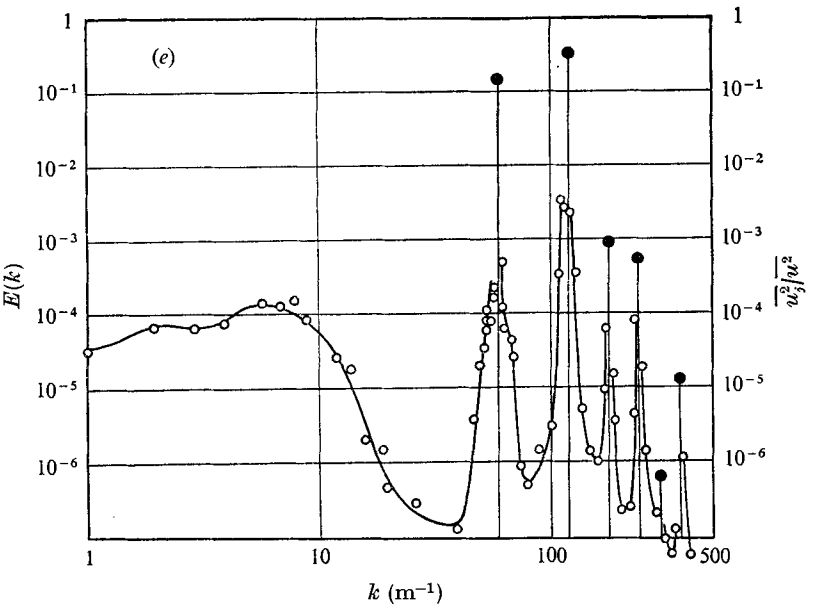

FIGURE 10. Energy spectra with 600 Hz sound. ●, line spectra $\overline{u_j^2}/\overline{u^2}$. $k = f/U_0$.

	(*a*)	(*b*)	(*c*)	(*d*)	(*e*)
X (mm)	150	400	800	1200	400
Y (mm)	4	4	4	6	0

increase in the low wavenumber component and 'fusion' of humps. The magnitude of the low wavenumber spectrum at this point is more than 100 times that at $X = 150$ mm. The fraction of the energy in the continuous spectrum at this point is about 60% of the total. At $X = 1200$ mm, $Y = 6$ mm the wave form of the fluctuation is very irregular as shown in figure 7 and the energy contained in the continuous spectrum is more than 95%. The spectrum shown in figure 10 (*d*) is free from humps and valleys. By comparing figures 10 (*c*) and (*d*) we notice that the smooth spectrum at $X = 1200$ mm is formed by the increase in the energy at valleys and the decrease at humps. The evolution of the continuous spectrum on the centre-line ($Y = 0$) is similar to that shown in figures 10 (*a*)–(*d*). Figure 10 (*e*) shows an example at $X = 400$ mm. Figures 10 (*b*) and (*e*), at different Y positions, are similar except for the dominant humps around the second and fourth harmonics in figure 10 (*e*). An example of a spectrum in natural transition is shown in figure 11 for comparison. In natural transition, line and continuous spectra are not distinguishable, although there are at least two peaks in the spectrum. By comparing figure 11 with figure 10 (*b*), we notice that the low wavenumber components in natural transition are much larger and figure 11 is closer to a turbulent spectrum. In other words, the transition to a turbulent spectrum is hampered by the presence of sinusoidal sound. A detailed discussion of this aspect will be given later.

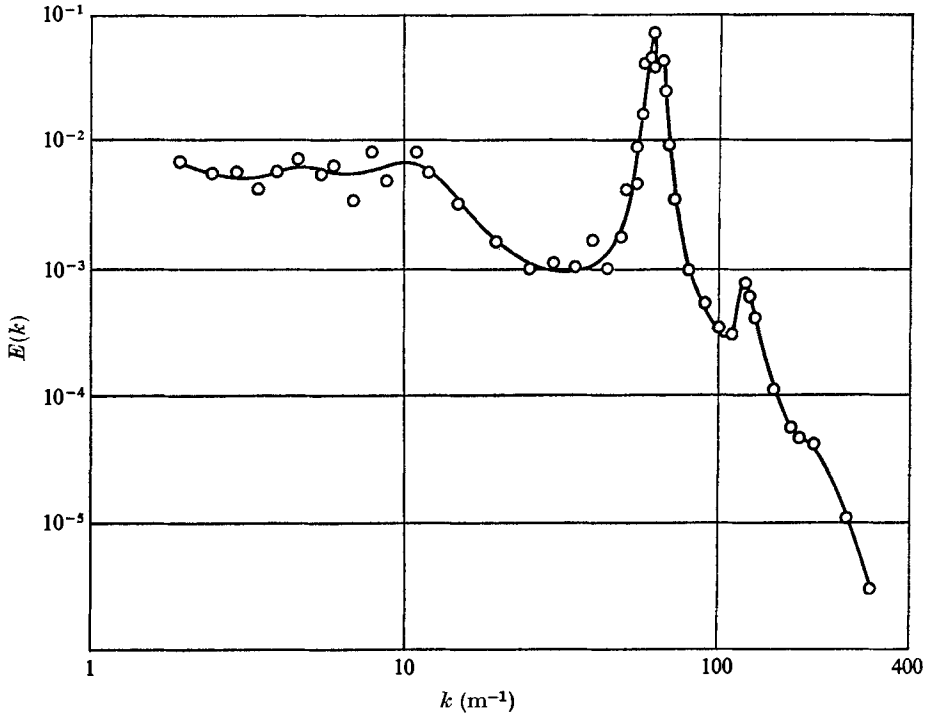

FIGURE 11. Energy spectrum at $X = 400$ mm, $Y = 4$ mm in natural transition.

4. Discussion

The mechanism of sound-induced transition seems to be different from that of natural transition. The difference stems from the nature of the initial disturbance. Natural transition is initiated by a random small amplitude fluctuation of a continuous energy spectrum. Since each spectral component of the fluctuation grows at a different rate, a peak is formed in the spectrum at the wavenumber with maximum growth rate as shown in figure 11. The nonlinear interaction between spectral components results in a smooth turbulent spectrum. When sound of a single frequency is introduced, both the induced sinusoidal fluctuation and natural fluctuation grow in the flow direction. While the amplitudes of the two fluctuations are small, they do not interact with each other. They grow independently and the spectrum consists of a discrete component and a continuous part. Figure 12 shows a comparison of two continuous spectra around $k = 60\,\mathrm{m}^{-1}$ in the linear region ($X = 20$ mm, $Y = 0{\cdot}5$ mm) for natural and sound-induced transitions. Both spectra are on the same scale and coincide very well. This proves that the growth of the natural fluctuation in the linear region is not affected by sound. The wave form here is sinusoidal with a slight modulation by random fluctuations as shown in figure 7. This modulated sinusoidal fluctuation is the 'output' from the linear region and the 'input' to the nonlinear region.

In the nonlinear region the growth of the fluctuation is no longer exponential and higher harmonics are produced. The even-order harmonics are intense near

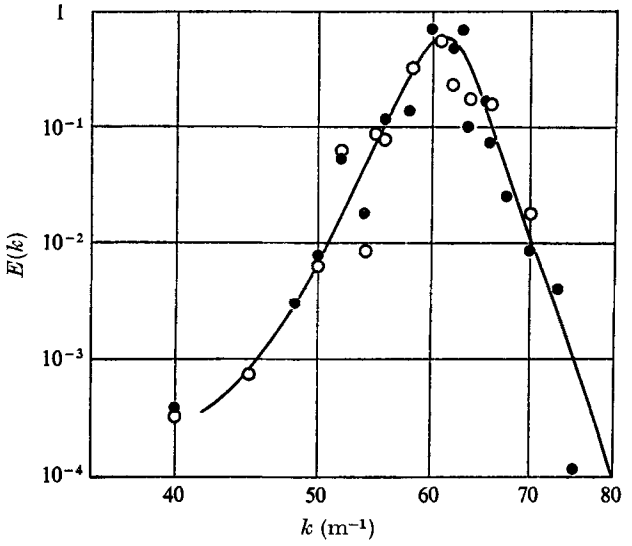

FIGURE 12. Energy spectra at $X = 20$ mm, $Y = 0{\cdot}5$ mm. ○, with 600 Hz sound; ●, natural transition. Scale of ordinate is arbitrary.

the centre-line, whereas odd-order harmonics are almost zero on the centre-line and maximum at certain off-centre points. These strong harmonic components interact with the weak random component. The extremely low level of the continuous spectrum shown in figure 10 (*b*) might be a consequence of this interaction. In a previous paper (Sato 1970) the suppression of the growth of a discrete spectral component by the presence of another strong discrete component was pointed out. Stuart (1962) demonstrated theoretically the possibility of suppression of the growth of one mode due to nonlinear interaction with another mode. Miksad (1973) observed mode suppression in the transition region of a separated shear layer. By comparing figures 10 (*b*) and 11 we notice that the continuous spectrum in sound-induced transition is an order of magnitude smaller. This fact indicates that the mutual 'growth suppression' takes place not only between discrete components but also between discrete and random components. If a strong and a weak component exist, the suppression is pronounced for the weak and slight for the strong component. The growth of components in humps around the fundamental component is high in the linear region but it is suppressed by the adjacent strong component in the nonlinear region. Components in valleys are very weak because of the low growth rate in the linear region and the suppression in the nonlinear region. The shape of spectra between $X = 150$ and 400 mm is explained by the first rule of nonlinear interaction; the growth of a spectral component is suppressed by the presence of other spectral components.

Figure 13 shows the spectrum at $X = 600$ mm, $Y = 4$ mm. If we compare this figure with figure 10 (*b*) at $X = 400$ mm, we notice a remarkable increase in low wavenumber regions. This increase continues until $X = 800$ mm (figure 10 *c*). This is another consequence of nonlinear interaction. The low wavenumber components might be produced by the interaction between high wavenumber

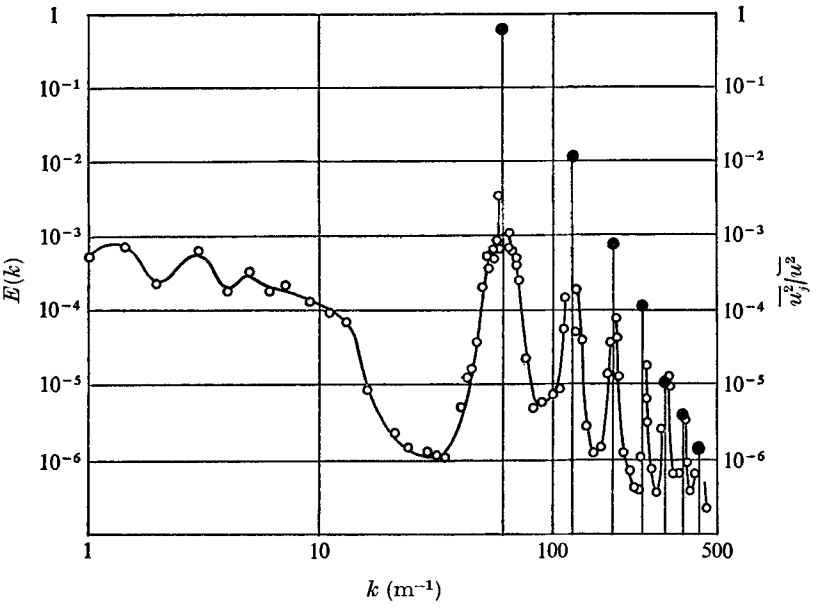

FIGURE 13. Energy spectrum at $X = 600$ mm, $Y = 4$ mm with 600 Hz sound. ●, line spectra $\overline{u_j^2}/\overline{u^2}$.

components and possibly between the discrete fundamental component and continuous components in humps around it. This process is analogous to the generation of low frequency components by the demodulation of a modulated high frequency signal.

A simple one-dimensional model of the process of producing a low frequency component out of high frequency components can be constructed as follows. By denoting non-dimensional velocity fluctuations at X and $X+\Delta X$ in the flow by $v_1 = u_1/U_0$ and $v_2 = u_2/U_0$, respectively, the nonlinear growth is expressed simply as

$$v_2 - v_1 = \Delta v = a_1 v_1 + a_2 v_1^2.$$

If $v_1 \ll 1$, $\Delta v = a_1 v_1$, namely, the growth is linear. The initial fluctuation with discrete and continuous components is expressed as

$$v_1 = A[1 + mp(t)] \sin 2\pi f_0 t,$$

in which A is the non-dimensional amplitude of the discrete component of frequency f_0, $p(t)$ is a random fluctuation with $\overline{p(t)} = 0$ and $\overline{p(t)^2} = 1$ and m represents the magnitude of the random part. Then v_2 becomes

$$v_2 = A(1+a_1)(1+mp)\sin 2\pi f_0 t + a_2 A^2[\tfrac{1}{2} + mp + \tfrac{1}{2}mp^2 - \tfrac{1}{2}(1 + 2mp + m^2p^2)\cos 4\pi f_0 t].$$

The first term is the linear part. By expressing $p^2(t)$ as

$$p^2(t) = 1 + q(t)$$

with $\overline{q(t)} = 0$, the nonlinear terms become

$$a_2 A^2[\tfrac{1}{2}(1+m^2)+mp+\tfrac{1}{2}m^2q-\tfrac{1}{2}(1+m^2+2mp+m^2q)\cos 4\pi f_0 t].$$

If $m \ll 1$, m^2q is neglected in comparison with $2mp$. Then, these terms become

$$\tfrac{1}{2}a_2A^2(1+m^2)+a_2A^2mp-\tfrac{1}{2}a_2A^2(1+m^2+2mp)\cos 4\pi f_0 t.$$

The first term is a d.c. component and represents the influence on the mean velocity, the second term is the random low frequency component and the last term corresponds to second harmonics modulated by random components. Since $p(t)$ is not correlated with $\sin 2\pi f_0 t$ and its harmonics, the energy spectrum of v_1 consists of a discrete component at $f = f_0$ and humps (side bands) $E(k-k_0)$ and $E(k_0-k)$ around it. On the other hand, the spectrum of v_2 includes a low frequency continuous part $E_p(k)$ which corresponds to $p(k)$. The magnitude of $E_p(k)$ depends on the value of a_2.

The validity of this simple model can be checked by comparing spectra at humps with $E_p(k)$. If they coincide, we can conclude that the low frequency portions of the spectra in figures 13 and 10 (*c*) are produced by the interaction of the fundamental and random components around it. Figure 14 (*a*) shows three spectra at $X = 600$ mm. They agree very well. The magnitude of $E_p(k)$ is shifted for the best agreement. Figure 14 (*b*) is another example at $X = 800$ mm. The agreement is also good.

The next question is why the process of producing low frequency components takes place around $X = 600$ mm rather than at smaller X. To answer this we introduce the second rule of nonlinear interaction: the nonlinear interaction producing components with sum and difference wavenumbers is more effective when the amplitudes of the interacting components are close. At small X discrete components are much stronger than the humps. The discrete components decay downstream as shown in figure 9. This decay is mainly due to energy transfer to the mean motion as has already been pointed out (Sato 1970). Because of the decay, the energy of the discrete components becomes closer to that at the humps and the interaction becomes more effective.

The persistence of deep valleys between humps at large X indicates that the nonlinear interaction between hump components of different harmonics is weak, because discrete components play no part in generating components at valleys. The filling-up of valleys is slow compared with the production of low wavenumber components. This fact leads us to the third rule of nonlinear interaction: the interaction is more effective for components with closer frequencies (wavenumbers). The filling-up of valleys may be accomplished by the generation of components whose wavenumbers are the sums of close low wavenumbers rather than by the production of components whose wavenumbers are the differences between high wavenumbers.

The evolution of the spectrum seems to be explained by the above-mentioned three fundamental rules, which are applicable to interactions between discrete components as well as between discrete and continuous components. The randomization process in sound-induced transition is the generation of a continuous

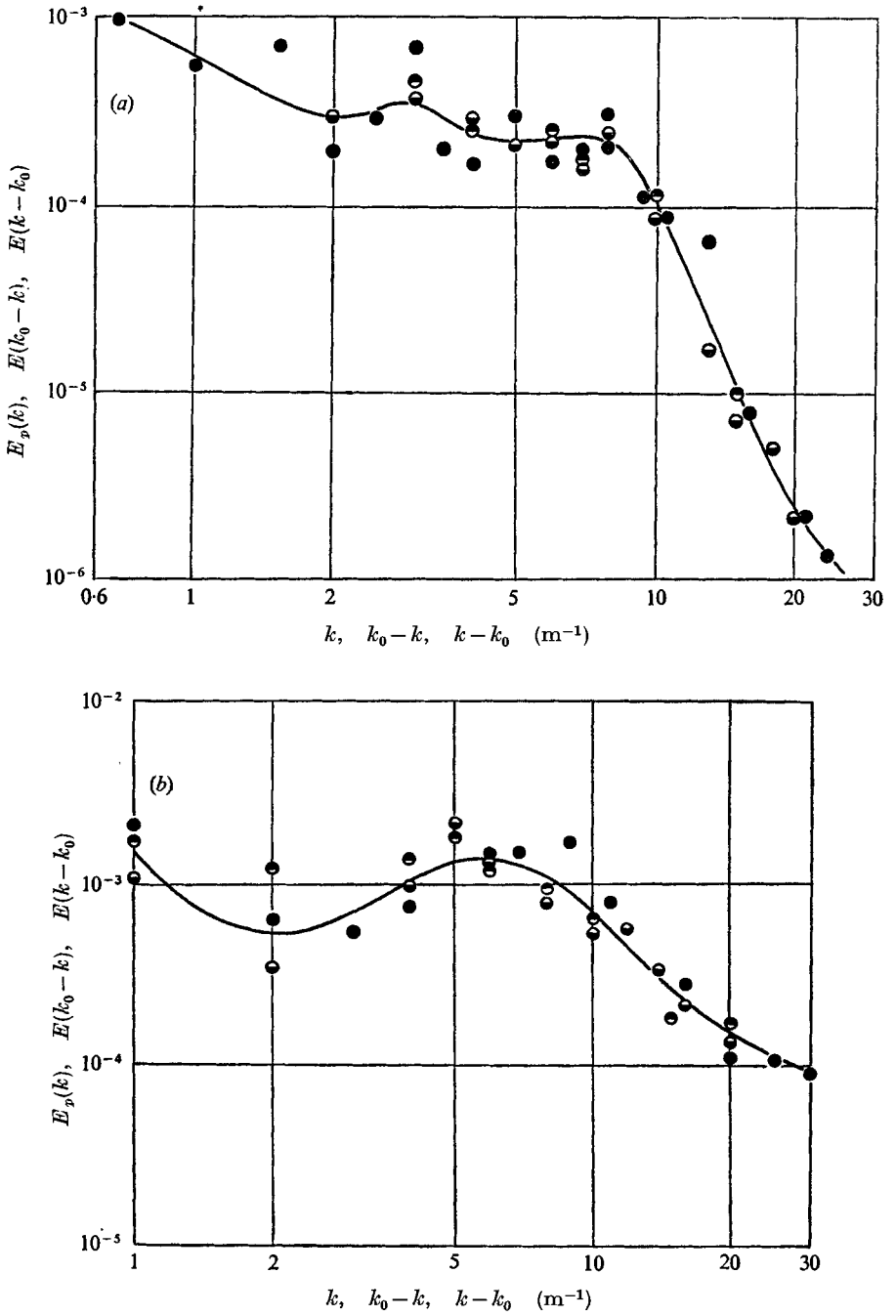

FIGURE 14. Spectra of modulating signal $E_p(k)$ at (*a*) $X = 600$ mm and (*b*) $X = 800$ mm, $Y = 4$ mm with 600 Hz sound. ●, direct measurement at low wavenumber; ◒, $E(k_0-k)$, lower side band; ◓, $E(k-k_0)$, upper side band.

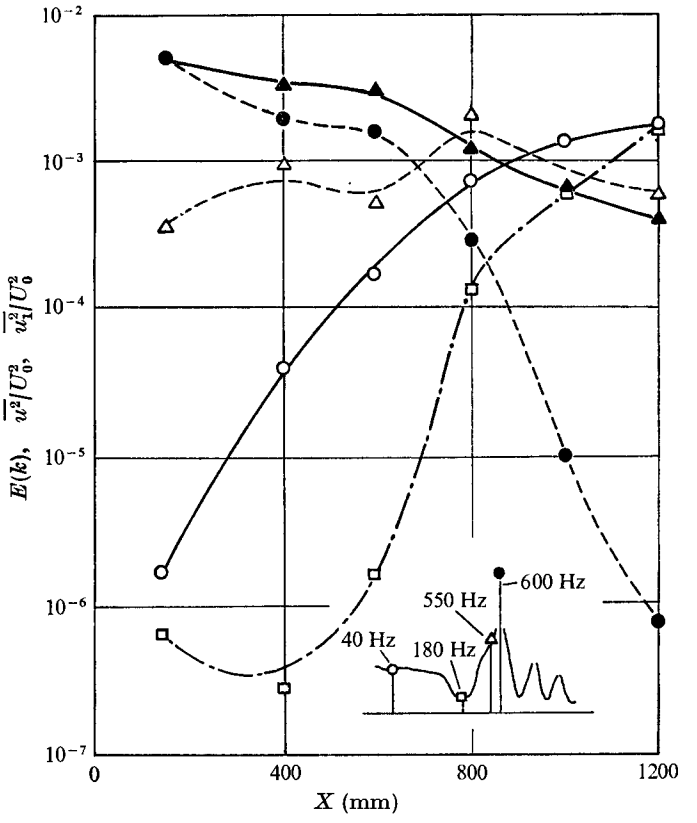

FIGURE 15. Streamwise variations of various spectral components along positions of maximum $\overline{u^2}$ at each X station. ▲, total energy $\overline{u^2}$; ●, line spectrum at 600 Hz; △, 550 Hz component; □, 180 Hz component; ○, 40 Hz component.

spectrum by the interaction between the energy-containing discrete components and the weak continuous spectrum.

The streamwise variations of the total energy and spectral components along lines of maximum $\overline{u^2}$ at each X station are shown in figure 15. The total energy $\overline{u^2}$ decreases gradually from $X = 150$ to 600 mm and rapidly further downstream. The decay of the fundamental discrete component (600 Hz, broken line) is most remarkable. The relative magnitudes of the three continuous spectral components are expressed correctly. The 550 Hz component, which represents the energy at a hump, does not change much. The component at a valley (180 Hz) starts increasing around $X = 600$ mm. The low frequency component (40 Hz) increases by a factor of almost 10^3 from $X = 150$ to 1200 mm. The reduction of $\overline{u^2}$ is mainly due to the decrease in the discrete components. Many components, but not the 40 Hz component, do not change much between $X = 150$ and 600 mm. This is an indication of the almost equilibrium nature of the region.

The degree of randomness of a fluctuation may be described by the 'randomness factor', defined as the ratio of the energy contained in the continuous spectrum to the total energy. The streamwise variation of the randomness factor

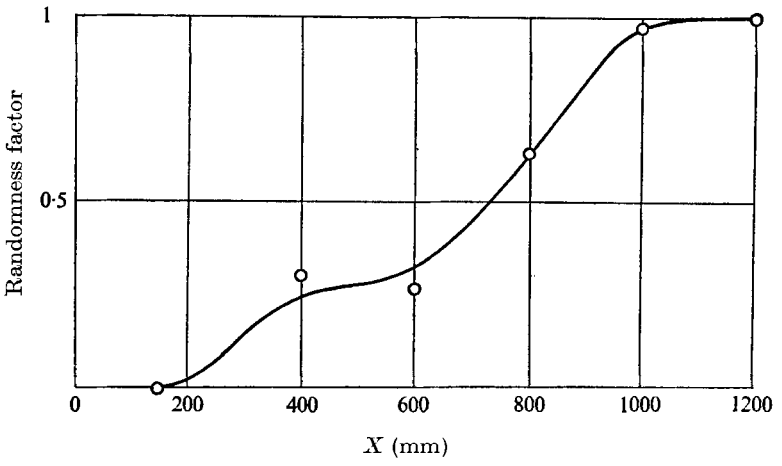

FIGURE 16. Streamwise variation of randomness factor along positions of maximum $\overline{u^2}$ at each X station with 600 Hz sound.

calculated from experimental data is shown in figure 16. This is the variation along lines of maximum $\overline{u^2}$ at each X station. The factor is zero at small X where the fluctuation is periodic. It starts increasing at around $X = 200$ mm, reaches 0·5 at about $X = 700$ mm and approaches one at $X = 1200$ mm. The region in which the randomness factor changes from zero to one may be called the randomization region and the randomization may be interpreted as the growth of the randomness factor. Figure 16 indicates the slow randomization process in the wake. The region of linear growth spans only 10–20 mm, in which amplification by a factor of more than 10^4 is accomplished, whereas the randomization region extends over 1000 mm. This is mainly due to the low-level residual disturbance in the free stream in contrast to the high-level discrete components. The effective nonlinear interaction takes place after the levels of the random and periodic components become comparable. Therefore, further reduction of the residual disturbance may result in a further delay in transition.

5. Conclusion

The following conclusions were obtained on the evolution of energy spectra during the transition process.

(*a*) As a result of nonlinear interactions an almost equilibrium state is established prior to the randomization of periodic fluctuations. The mean-velocity distribution, the fluctuation energy and the spectrum in this equilibrium region change very little in the flow direction.

(*b*) The growth and decay of discrete harmonic components are not monotonic although all harmonics disappear eventually in the fully developed turbulent wake.

(*c*) The first stage of the evolution of the continuous spectrum is the generation of low wavenumber components by the interaction of a discrete component and

continuous part around it (hump). The process is analogous to the demodulation of a modulated signal and a simple model explains the generation.

(*d*) The second stage is the decay of humps accompanied by the filling-up of valleys between humps.

(*e*) Three fundamental rules seem to be useful for explaining the interaction between periodic and random spectral components. They are: (i) the growth of a spectral component is suppressed by the presence of other strong components, (ii) components whose wavenumbers are the sum and difference of two wavenumbers are produced at a higher rate when the amplitudes of two interacting components are closer, and (iii) the interaction is more effective for components with closer wavenumbers.

(*f*) The randomness factor is defined as the ratio of the energy contained in the continuous spectrum to the total energy. It increases in the flow direction and the region in which it changes from zero to unity may be called the randomization region.

(*g*) Transition is delayed by the presence of sinusoidal sound.

REFERENCES

Browand, F. K. 1966 An experimental investigation of the instability of an incompressible, separated shear layer. *J. Fluid Mech.* **26**, 281.

Klebanoff, P. S., Tidstrom, K. D. & Sargent, L. M. 1962 The three-dimensional nature of boundary-layer instability. *J. Fluid Mech.* **12**, 1.

Lashinsky, H. 1968 *Proc. Symp. on Turbulence of Fluid & Plasmas*, p. 29. New York: Polytechnic Press.

Miksad, R. W. 1972 Experiments on the nonlinear stages of free-shear-layer transition. *J. Fluid Mech.* **56**, 695.

Miksad, R. W. 1973 Experiments on nonlinear interactions in the transition of a free shear layer. *J. Fluid Mech.* **59**, 1.

Sato, H. 1959 Further investigation on the transition of two-dimensional separated layer at subsonic speeds. *J. Phys. Soc. Japan*, **14**, 1797.

Sato, H. 1970 An experimental study of non-linear interaction of velocity fluctuations in the transition region of a two-dimensional wake. *J. Fluid Mech.* **44**, 741.

Sato, H. & Kuriki, K. 1961 The mechanism of transition in the wake of a thin flat plate placed parallel to a uniform flow. *J. Fluid Mech.* **11**, 321.

Stuart, J. T. 1962 *Proc. Int. Congr. Appl. Mech., Stresa*, p. 63. Elsevier.